2011 50th IEEE Conference on Decision and Control and
European Control Conference (CDC-ECC)
Orlando, FL, USA, December 12-15, 2011

Spectral Analysis of sEMG Signals to Investigate Skeletal Muscle Fatigue

Parmod Kumar, Anish Sebastian, Chandrasekhar Potluri, Yimesker Yihun, Madhavi Anugolu, Jim Creelman, Alex Urfer, D. Subbaram Naidu, *Fellow, IEEE,* and Marco P. Schoen, *Senior Member, IEEE*

Abstract— **Our recent investigations are focused to develop dynamic models for skeletal muscle force and finger angles for prosthetic hand control using surface electromyographic sEMG as input. Since sEMG is temporal and spatially distributed and is influenced by various factors, muscle fatigue and its related sEMG becomes of importance. This study is an effort to spectrally analyze the sEMG signal during progression of muscle fatigue. The sEMG is captured from the arms of healthy subjects during muscle fatiguing experiments for dynamic and static force levels. Filtered sEMG signal is segmented in five parts with 75% overlap between adjacent segments. The analysis is done using different classical (fast Fourier transform, Welch's averaged modified periodogram), model-based (Yule-Walker, Burg, Covariance and Modified Covariance autoregressive (AR) method), and eigenvector methods (Multiple Signal Classification (MUSIC) and eigenvector spectral estimation method) in frequency domain. Results show that the classical and eigenvector based methods are more sensitive than the model-based methods to fatigue related changes in sEMG signals.**

I. Introduction

THIS work focuses on the analysis of sEMG signals, which are electric voltages ranging between -5 to +5 mV and investigates the effects of fatigue in the skeletal muscles. The motor units operate as a consequence of the central nervous system control strategies, signal transmission along nerve fibers and across neuromuscular junctions, electrical activation of the muscle fibers organized in elementary motors and, through a chain of complex biochemical events. The productions of the forces acting on the tendons of the agonist and/or antagonist muscles predict bone movement [1]. This mechanism also involves a number of feedback circuits relaying back to the spinal cord and the brain information concerning the length and velocity of shortening of the muscles and the forces acting on the tendons [1]. The EMG signal gives information about the motor points and their controller i.e. the central nervous system [2, 3]. The central nervous system activates and controls the EMG signals which depend on the flow of specific ions including sodium (Na^{+}), potassium (K^{+}) and calcium (Ca^{++}) resulting in the action potentials in nerves and their respective skeletal muscle fibers from which EMG signals are derived. Research efforts in the last few decades have focused on the prosthetic design where sEMG is a control input to activate the prosthesis. The sEMG is a dynamic signal with continual change in its pattern and strength and this becomes more complex with the fatigue induced in skeletal muscles.

Failure to maintain the required force level is termed as muscle fatigue, which is a complex phenomenon [4]. Reasons for fatigue can be the result of peripheral changes at the muscle level or an inadequate output from the central nervous system to stimulate motoneurons [4]. Intricacies of muscle fatigue are associated with several aspects where the relative importance of each depends on the fiber type and composition of the contracting muscle(s), as well as the intensity, type, and duration of contraction activity. Muscle cells are the focal points of fatigue and rarely involve the central nervous system or the neuromuscular junction [5]. The amount of force generated, duration of each contraction, and the rest period between two contractions has a direct influence on the muscle fatigue rate [6]. Muscle fiber-type distribution [7, 8], nerve conduction velocity of fatiguing muscles [9, 10], or even central factors within the central nervous system (CNS) will affect motivation to perform activities [11]. The EMG analysis is a well-accepted method for muscle fatigue assessment [8-10, 12-17]. Even though the sEMG has some limitations associated with the skin impedance, electrode placement, and cross-talk, it is used for the estimation of muscle fatigue of different muscles [16, 18, 19].

L. Lindstrom et al. developed a method that measures the localized muscle fatigue based on the power spectrum analysis using myoelectric signals, [20]. This approach permits real-time investigations and can yield statistically based criteria for the occurrence of fatigue. Rate of fatigue development and changes in muscle action potential conduction velocity were used to interpret the findings [20-22]. Additional recruitment of motor units, synchronization

Manuscript received March 22, 2011. This work was supported in part by the US Department of the Army, under the award number W81XWH-10-1-0128.

Parmod Kumar is with Measurement and Control Engineering Research Center (MCERC), School of Engineering, Idaho State University, Pocatello, Idaho 83209, USA (email: kumaparm@isu.edu).

Anish Sebastian, Chandrasekhar Potluri, Yimesker Yihun, and Madhavi Anugolu are with MCERC, School of Engineering, Idaho State University, Pocatello, Idaho 83209, USA (e-mail: sebaanis@isu.edu, potlchan@isu.edu, yihuyime@isu.edu, anugmadh@isu.edu).

Jim Creelman and Alex Urfer are with Department of Physical and Occupational Therapy, Idaho State University, Pocatello, Idaho 83209, USA (email: creejame@isu.edu, urfealex@isu.edu).

D. Subbaram Naidu is with Department of Electrical Engineering and Computer Science, MCERC, Idaho State University, Pocatello, Idaho 83201 USA (email: naiduds@isu.edu).

Marco P. Schoen is with Department of Mechanical Engineering, MCERC, Idaho State University, Pocatello, Idaho 83209, USA (email: schomarc@isu.edu).

of active motor units along the muscle fibers, and a decrease in conduction velocity is reflected in the EMG signal as an increase of amplitude in time domain and a decrease of medium frequency in frequency domain [23, 24].

The joint analysis method using sEMG amplitude and spectrum (JASA) allows distinguishing between the difference of fatigue-induced and force related EMG changes. Simultaneous changes in the EMG amplitude and spectrum is considered in the JASA approach [25]. According to traditional measurements, the EMG amplitude increases and median frequency (MF) decreases as a result of muscle fatigue [26-28]. Fatigue can occur because of continuous high frequency and tetanic stimulations. Decline in the force magnitude can be attributed to reduced Ca^{++} release from the sarcoplasmic reticulum (SR), reduced myofibrilllar Ca^{++} sensitivity, or because of reduced maximum Ca^{++}– activated tension. The main reason of the tension decline with continuous tetanic stimulation is decreased Ca^{++} release, which is due to impaired action potential propagation in the T tubules. Decrease in pH and increase in inorganic phosphate (Pi) concentration causes reduced Ca^{++} sensitivity and decline in maximum tension. This is the main contributing factor in decline of force with continual tetanic stimulation [29].

Increase in the inorganic phosphate in the myoplasm ([Pi]myo) results in reduced SR Ca^{++} release in both skinned and intact fibers. Muscle performance declines with rigorous activities which results in fatigue. Metabolic changes on either the contractile machinery or the activation process are also responsible for the fatigue of muscles. Myofibrillar proteins and activation process both are affected during fatigue with substantial increase in the concentration of inorganic phosphate (Pi) in myoplasm. Further, it has been shown that failure of the sarcoplasmic reticulum (SR) to release Ca^{++} also contributes to fatigue [30]. During intense exercise of skeletal muscles (less than 20 seconds), cells consume 100 of times more energy than during the rest period. The aerobic capacity of muscle cells falls short on energy demand and anaerobic metabolism must supply the majority of the adenosine triphosphate (ATP) required. Skeletal muscle fatigue results because of the high-intensity exercise. Hence, the anaerobic metabolism pathway results in a decline of contractile functionality [31].

The present work investigates the change in sEMG in frequency domain during skeletal muscle fatigue. The sEMG signals are acquired for multiple subjects for dynamic and static force experiments to induce skeletal muscle fatigue. The sEMG signals are filtered with a nonlinear Teager–Kaiser Energy (TKE) operator-based nonlinear spatial filter [32]. Two sets of dynamic force data are segmented into three and five parts and two sets of static force data are segmented into five parts each. There is a 75% overlap between the two adjacent segments. A number of classical, model-based and eigenvector based spectral estimation techniques are used to study the change in the sEMG signals as a result of muscle fatigue. In classical methods Fast Fourier transform (FFT) and Welch's averaged modified periodogram methods are used. In case of model-based methods Yule-Walker (Y-W), Burg, Covariance (Cov.) and Modified Covariance (Mcov.) Autoregressive (AR) methods are applied. For eigenvector methods Multiple Signal Classification (MUSIC) and Eigenvector (EIG) spectral estimation methods were selected for processing sEMG signals. Using these spectrum analysis techniques, Power Spectral Density (PSD) estimates and detailed documentations of the sEMG signals were obtained. These methods were compared in terms of their frequency resolution and the effects in determination of skeletal muscle fatigue.

II. Experimental Set-Up And Pre-Processing

An experiment set-up was developed using DELSYS® Bagnoli-16 EMG system with nine DE-3.1 sEMG sensors to capture the sEMG signals from skeletal muscles as given in [32]. This arrangement involves nine sensors covering four directional spatial distributions of the sEMG signal. The appropriate motor point of the flexor digitorum superficialis muscle (FDS), which controls the flexion of the ring finger, was identified using a wet probe muscle stimulator at the FDS (RICH-MAR, HV 1000). The middle three sEMG sensors were attached directly on the skin surface above the motor point of the ring finger. Prior to placing the sEMG sensors, the skin surface of the subject was prepared according to International Society of Electrophysiology and Kinesiology (ISEK) protocols [33]. Two different sets of fatigue inducing experiments were conducted using this set-up of sEMG sensors. One experiment using dynamic force variations and another with 50 pounds of static force. For the dynamic force variation we used an Interlink™ Electronics FSR 0.5" circular force sensor on a stress ball and for the static force experiment we used a cable tensionmeter (T5166) by 'Pacific Scientific Company.'

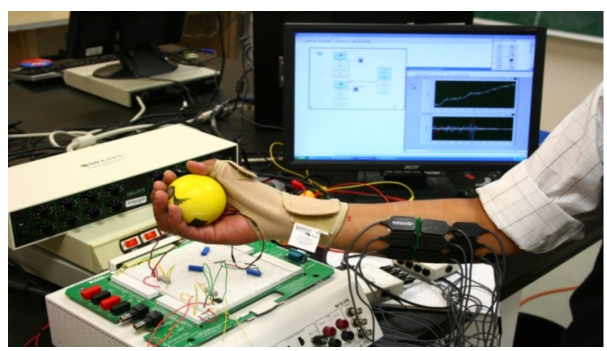

Fig. 1. Experimental set-up for dynamic force levels.

For the dynamic force experiment we restricted the thumb movement using a thumb splint. For the static force experiment we held the force of the dynamometer at 50 pounds and tried to maintain this force level to induce fatigue in skeletal muscles. Force data for dynamic force experiments was captured using NI ELVIS™ with Interlink™ Electronics FSR 0.5" circular force sensor. Experimental set-up is shown in Fig. 1 and 2, where 9 sensors are shown on a healthy subject forearm, holding a stress ball and a grip tension dynamometer, respectively. The sEMG and finger force data was collected at a sampling rate of 2000 Hz using LabVIEW™ in conjunction with DELSYS® Bagnoli-16 EMG and NI ELVIS™. With these experimental set-ups, we conducted several experiments of 30 seconds, 45 seconds and 60 seconds durations.

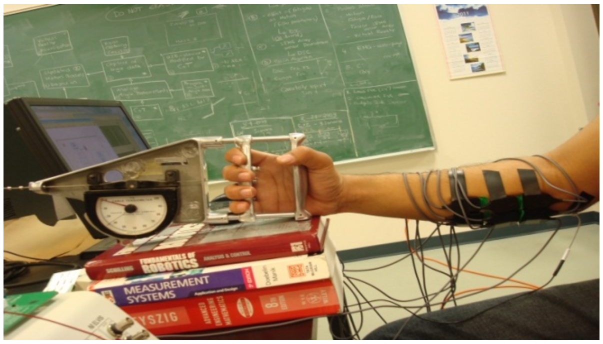

Fig. 2. Experimental set-up for 50 pounds static force levels.

III. Spectral Estimation Methods

Signals can be analyzed in the time and frequency domains and in some instances the frequency content of the signal is more useful than the time domain characteristics [34]. Various bio signals such as the heart rate, EMG, EEG, ECG, eye movements, and other motor responses, acoustic heart sounds, and stomach and intestinal sounds, show much richer information in the frequency domain [34]. Spectral analysis is a mathematical prism which finds the frequency content of a waveform by decomposing the signal into its constituent frequencies [34, 35]. There is a wide range of methods for spectral analysis, each having its own benefits and drawbacks. In this research we are using classical methods based on the Fourier transform, modern methods based on the estimation of model parameters, and eigenvector based methods [34] in order to characterize the muscle fatigue occurring in skeletal human muscles, in particular muscles of the forearm. To use the spectral analysis wisely, we need to have an understanding of the spectral features of interests and the best methods to accurately determine those features [34].

A. Discrete Fourier Transform (DFT)

DFT which is the computational basis of the spectral analysis transforms the time or space domain data into frequency domain data [36]. The DFT of a vector x of length N is given as

$$X(k) = \sum_{j=1}^{N} x(j)\omega_N^{(j-1)(k-1)}, \tag{1}$$

where $\omega_N = e^{(-2\pi i)/N}$ is the N_{th} root of unity [36].

B. Welch's averaged modified periodogram method:

As the name suggests, the 'Welch's averaged modified periodogram method' depends on the periodogram of the signal $\{x(n)_n^N\}$ which is given by Equation (2), [36].

$$\hat{S}_{per}(f) = \frac{1}{N}\left|\sum_{n=1}^{N} x(n)\exp(-j2\pi f n)\right|^2. \tag{2}$$

In Welch method, the signal is segmented into eight parts of equal length with an overlapping ratio of 50% and each part is segmented using a Hamming window as given by Equation (3), [36].

$$w(n) = 0.54 - 0.46\cos\left(2\pi\frac{n}{N}\right), 0 \le n \le N\ . \tag{3}$$

C. Yule-Walker (Y-W) autoregressive (AR) method:

The Yule-Walker autoregressive method, also called the autocorrelation method, estimates the power spectral density (PSD) of the input. This method fits an autoregressive (AR) model to the windowed input data by minimizing the forward prediction error in the least-squares sense. This formulation leads to the Yule-Walker equations, which are solved by Levinson-Durbin recursion [36].

D. Burg autoregressive (AR) method:

The Burg autoregressive (AR) method is a parametric spectral estimation method of the signal, x. The power spectral density is calculated in units of power per radians per sample. This method is based on the minimization of the forward and backward prediction error and on estimation of the reflection coefficients [36].

E. Covariance (Cov.) autoregressive (AR) method:

The covariance autoregressive (AR) method uses the covariance algorithm to estimate the parametric spectral density of the signal, x. Based on causal observation of the input signal, the covariance method minimizes the forward prediction error and fits an AR linear prediction filter model to the signal [36].

F. Modified covariance (Mcov.) autoregressive (AR) method:

Modified covariance autoregressive (AR) method estimates the PSD of the signal using the modified covariance method. Based on the causal information of the input signal, the modified covariance method fits an autoregressive (AR) linear prediction filter model to the signal by simultaneously minimizing the forward and backward prediction errors. The spectral estimate returned by this method is the magnitude squared frequency response of the AR model [36].

G. Multiple Signal Classification (MUSIC) spectral estimation method:

The MUSIC algorithm estimates the pseudospectrum (in rad/sample) at the corresponding vector of frequencies for the input signal x [36]. This algorithm uses the estimates of the eigenvectors of a correlation matrix associated with the input signal using Schmidt's eigenspace analysis method [37]. The MUSIC pseudospectrum estimate is given by Equation (4),

$$P_{music}(f) = \frac{1}{e^H(f)\left(\sum_{k=p+1}^{N} v_k v_k^H\right)e(f)} = \frac{1}{\sum_{k=p+1}^{N}\left|v_k^H e(f)\right|^2}, \tag{4}$$

where N is the dimension of the eigenvectors and v_k is the k-th eigenvector of the correlation matrix [36]. The signal subspace has a dimension p and the eigenvectors v_k used in the sum corresponds to the smallest eigenvalues and also spans the noise subspace [36]. The vector $e(f)$ consists of the complex exponentials, so the inner product $v_k^H e(f)$ amounts to a Fourier transform. To estimates the pseudospectrum, the squared magnitudes are summed for FFT computed for each v_k [36].

H. Eigenvector (EIG) spectral estimation method:

The eigenvector spectral estimation method estimates the pseudospectrum (in rad/sample) at the corresponding vector of frequencies using estimates of the eigenvectors of a correlation matrix associated with the input signal x [36]. This method estimates the pseudospectrum from a signal or a correlation matrix using a weighted version of the MUSIC algorithm derived from Schmidt's eigenspace analysis method [37, 38]. To find the frequency content of the signal the algorithm performs eigenspace analysis of the signal's correlation matrix. Singular value decomposition is used to compute the eigenvalues and eigenvectors of the signal's correlation matrix [36]. This method computes the pseudospectrum estimate as given by Equation (5).

$$P_{ev}(f) = \frac{1}{\left(\sum_{k=p+1}^{N} \left|v_k^H e(f)\right|^2\right)/\lambda_k}, \tag{5}$$

where the eigenvectors have a dimension of N and v_k is the k-th eigenvector of the correlation matrix [36]. The signal subspace has a dimension p and the eigenvectors v_k used in the sum corresponds to the smallest eigenvalues and also spans the noise subspace [36]. The vector $e(f)$ consists of the complex exponentials, so the inner product $v_k^H e(f)$ amounts to a Fourier transform and to estimate the pseudospectrum, the squared magnitudes are summed for FFT computed for each v_k [36].

I. Selection of Model Orders for Model-Based and Eigenvector Based Methods

Model-based and eigenvector-based methods need to have a specific model order which is an important aspect of the use in these methods. Using the sEMG and force data as input and outputs for three and five sets of the segments for different data sets, we created model structure matrices using 'struc' function in MATLAB®, using 'arxstruc' we compared a model order of 1 to 50th with varying delay of 1 to 50 using cross-validation on the second half of the data set. With this approach, it was possible to select the order that gives the best fit for the validation data set.

IV. Results and Discussion

sEMG signal changes as a consequence of muscle fatigue [23-28], the amplitude of the PSD of the signal increases and the median frequency shifts towards the lower frequency range [26-28]. In this study, PSDs of the different segments of each sEMG data set were obtained using FFT, Welch's averaged modified periodogram, Yule-Walker, Burg, Covariance, Modified Covariance autoregressive (AR), Multiple Signal Classification (MUSIC), and Eigenvector spectral estimation methods. The objective of this study was to determine preferred methods of signal processing that elevates the sensitivity of muscle fatigue as represented in the PSD of the sEMG signal. An increased sensitivity allows for better modeling of the fatigue phenomena and hence more accurate sEMG models. Ultimately this may lead to better prosthetic control.

Data of two experiments for dynamic force variations was segmented in three and five parts respectively. Each segment is with an overlap of 75% with its adjacent segment. Using different methods, we computed the PSDs for each segment. For the dynamic force experiments, the maximum value of PSDs of sEMG signal increases with muscle fatigue as time or segment number is increased. The classical methods (FFT and Welch) and eigenvector based methods (MUSIC and Eigenvector (EIG.)) are representing this change well in case of maximum PSD values and show a clear difference.

Table I lists the peak values of the PSDs of five segments using classical and eigenvector based methods for a dynamically varying force experiment. Fig. 3 shows the overlapping plot of PSDs for five segments using the MUSIC algorithm based spectral estimation method. The increase in the maximum PSD value is evident from the 1st to the 5th segment of the data.

TABLE I
MAXIMUM VALUE OF PSD FOR CLASSICAL METHODS AND EIGENVECTOR BASED METHODS – DYNAMIC VARYING FORCE – EXPERIMENT 2

Segment No.	Classical-Methods		Eigenvector-Methods	
	FFT	Welch	MUSIC	EIG
1st	4.1e+6	0.0082	371.59	1.0819
2nd	5.09e+6	0.0100	424.43	1.3892
3rd	5.74e+6	0.0111	480.71	1.4132
4th	6.79e+6	0.0133	508.64	1.4936
5th	2.13e+7	0.0379	695.08	10.2118

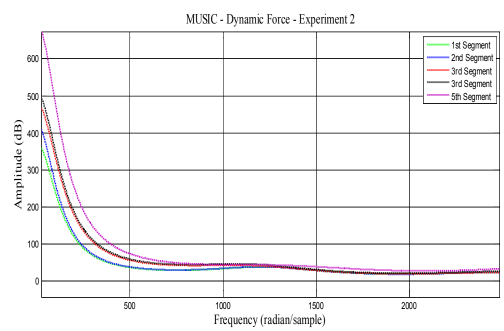

Fig. 3. PSD vs. Frequency Plot for MUSIC Algorithm – Dynamic Force Experiment.

Fig. 4 shows the resulting PSD using the Burg method. Comparing Fig. 3 and 4, the progression of fatigue influence shift in PSDs is evident in both plots. However, the MUSIC algorithm not only shows larger amplitudes, but also a greater relative sensitivity to fatigue.

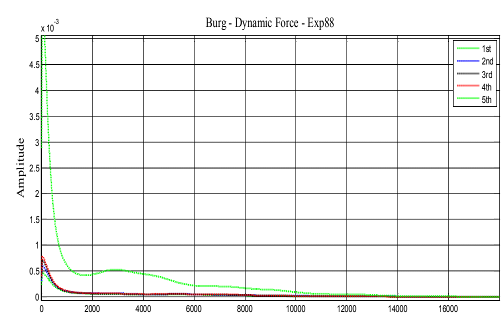

Fig. 4. PSD vs. Frequency Plot for Burg Method – Dynamic Force Experiment.

The rather equal spacing between the lines of the PSD for the MUSIC algorithm compared to the Burg method indicates a rather more linear relationship of the fatigue progression.

The sEMG data of two experiments for static force (50 pounds) were processed and the maximum PSDs of five segments using classical, model-based, and eigenvector based methods were computed. Data from both the experiments show similar results as the dynamic case. Table II lists the peak values of the PSDs of five segments using classical and eigenvector based methods for static force (50 pounds) for one experiment. Table III lists the maximum values of the PSD for model-based methods: Y-W, Burg, Covariance, and modified covariance.

TABLE II
MAXIMUM VALUE OF PSD FOR CLASSICAL METHODS – STATIC FORCE – 50 POUNDS - EXPERIMENT 1

Segment No.	Classical-Methods		Eigenvector-Methods	
	FFT	Welch	MUSIC	EIG
1st	1.03e+5	6.81e-5	1413	9.93e-4
2nd	1.80e+5	1.12e-4	1793	16e-4
3rd	3.21e+5	1.80e-4	2296	28e-4
4th	4.25e+5	2.62e-4	3102	37e-4
5th	6.23e+5	3.58e-4	7723	104e-4

TABLE III
MAXIMUM VALUE OF PSD FOR CLASSICAL METHODS – STATIC FORCE – 50 POUNDS - EXPERIMENT 1

Segment No.	1st	2nd	3rd	4th	5th
Model-Based Methods	7.7e-7	1.3e-6	2.3e-6	3.1e-6	7.81-6

All of these methods resulted in the same maximum values for each segment. Comparing Table II and III, we recognize the large difference in maximum value between the model-based methods and the corresponding values from the FFT and MUSIC method. Fig. 5 shows the overlapping plot of PSDs for five parts using eigenvector algorithm based spectral estimation method. The increase in the maximum PSD value is evident from the 1st to the 5th segment of the static force sEMG data.

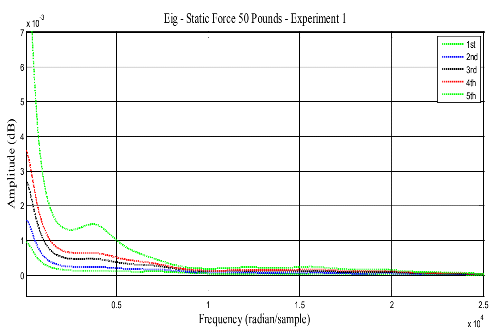

Fig. 5. PSD vs. Frequency Plot for Eigenvector Method – Static Force of 50 Pounds.

The eigenvector method produces a similar characteristic as the MUSIC algorithm and distinguishes itself by also providing a more linear characteristic of the fatigue progression and a greater relative sensitivity. Fig. 6 depicts the PSD generated by using FFT method for the 1st and 5th segments of a static force experiment. While providing a large maximum value, the FFT method is limited by its own spectral resolution ($1/N$) and, due to windowing of the finite data set, results into spectral leaking.

All the model-based methods for both dynamic and static force levels produce the same peak values and the same PSD for the corresponding experiment. Since Burg and Y-W methods guarantee stability while the covariance and modified covariance methods have conditions for stability to be satisfied (i.e. min. order must be of certain length of the input frame size), Burg and Y-W should be the preferred methods for sEMG analysis. However, the Burg method is to be preferred if short data sets are used.

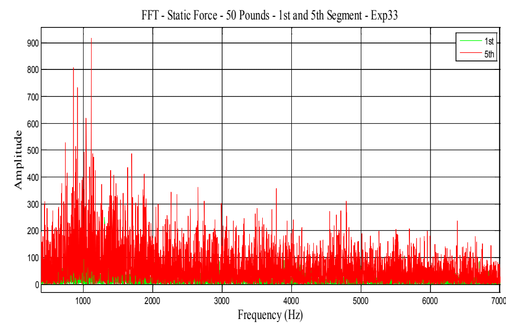

Fig. 6. PSD vs. Frequency Plot for FFT Method – Static Force of 50 Pounds.

Comparing the eigenvector based methods (MUSIC and Eigenvector), both of these methods are frequency estimator techniques based on eigenanalysis of the autocorrelation matrix where the resulting estimate has sharp peaks at the frequencies of interest. The eigenvector method uses inverse eigenvector weighting whereas the MUSIC method uses unity weighting, implying that the eigenvector method gives fewer spurious peaks than the MUSIC algorithm [39]. As seen from the dynamic experiment results, the MUSIC method provides for a better spacing between the segment based PSDs compared to the Burg and eigenvector method. From static experiments, we conclude that all three (MUSIC, Burg, and Eigenvector) methods perform similarly if a linear relationship of the fatigue progression is desired.

V. Conclusion and Future Work

This research characterizes muscle fatigue using a PSD representation of different segments of sEMG data. Classical (fast Fourier transform and Welch's averaged modified periodogram), model-based (Y-W, Burg, Cov., and Mcov. autoregressive (AR) method) and eigenvector based methods (MUSIC and EIG. spectral estimation method) are used to compute the PSDs. Classical and eigenvector based methods are more sensitive than the model-based methods for analyzing the fatigue related changes in sEMG signal. However, the MUSIC algorithm provides good maximum value in the PSD as well as a clear distinction between the segmented sEMG data. The latter point is indicative of a relative linear fatigue progression in time for the same case when the MUSIC algorithm is utilized. In the future work these results can be used to design and improve the skeletal muscle 'Force-sEMG-Fatigue' based models [40] for prosthetic design and other rehabilitation research.

ACKNOWLEDGMENT

This research was sponsored by the US Department of the Army, under the award number W81XWH-10-1-0128 awarded and administered by the U.S. Army Medical Research Acquisition Activity, 820 Chandler Street, Fort Detrick MD 21702-5014. The information does not necessarily reflect the position or the policy of the Government, and no official endorsement should be inferred. For purposes of this article, information includes news releases, articles, manuscripts, brochures, advertisements, still and motion pictures, speeches, trade association proceedings, etc.

REFERENCES

[1] R. Merletti, and P. Parker, "ELECTROMYOGRAPHY: Physiology, Engineering, and Noninvasive Applications," John Wiley & Sons, Inc., Hoboken, New Jersey, 2004, ch. 1.
[2] Merletti, R., D. Farina, M. Gazzoni, A. Merlo, P. Ossola, and A. Rainoldi, "Surface electromyography: A window on the muscle, a glimpse on the central nervous system," Europa Medicophysica 37, 57–68 (2001).
[3] Wolf, W., "The EMG as a window to the brain: signal processing tools to enhance the view," in I. Gath, and G. Inbar, eds., Advances in processing and pattern analysis of biological signals, Plenum Press, New York, 1996, pp. 339–356.
[4] S. C. Gandevia, 2001. "Spinal and Supraspinal Factors in Human Muscle Fatigue". Physiological Reviews, American Physiological Society 81(4), October.
[5] R. H. Fitts, 1994. "Cellular mechanisms of muscle fatigue". Physiological Reviews, American Physiological Society, 74, pp. 49-94.
[6] B R Bigland-Ritchie, N J Dawson, R S Johansson and O C Lippold, 1986. "Reflex origin for the slowing of motoneurone firing rates in fatigue of human voluntary contractions". Journal of Physiology, 379, pp. 451-459.
[7] Gerdle B, Edstrom M, Rahm M, 1993." Fatigue in the shoulder muscles during static work at two different torque levels". Clinical Physiology, 13(5), pp. 469-482.
[8] Paavo V. Komi, and Per Tesch, 1979. "EMG frequency spectrum, muscle structure, and fatigue during dynamic contractions in man". European Journal of Applied Physiology, 42(1), pp. 41-50.
[9] M. Hagberg, 1981. "Muscular endurance and surface electromyogram in isometric and dynamic exercise". Journal of Applied Physiology, 51, pp. 1-7.
[10] M. Hagberg, 1981. "Electromyographic signs of shoulder muscular fatigue in two elevated arm positions". American Journal of Physical Medicine, 60(3), pp.111-121.
[11] Enoka RM, 1995. "Morphological features and activation patterns of motor units". Journal of Clinical Neurophysiology, 12(6), pp. 538-559.
[12] L. G. Christova, A. S. Alexabdrov, and B. A. Ishpekova, 1999. "Single motor unit activity pattern in patients with Schwartz-Jampel syndrome". Journal of Neurology, Neurosurgery and Psychiatry, 66(2), pp. 252-253.
[13] Björn Gerdle, Jessica Elert, and Karin Henriksson-Larsén, 1989. "Muscular fatigue during repeated isokinetic shoulder forward flexions in young females". European Journal of Applied Physiology, 58(6), pp. 666-673.
[14] Paula M. Ludewig, and Thomas M. Cook, 1996. "The effect of head position on scapular orientation and muscle activity during shoulder elevation". Journal of Occupational Rehabilitation, 6(3), pp. 147-158.
[15] Merletti R, and Lo Conte LR, 1997. "Surface EMG signal processing during isometric contractions". Journal of Electromyography and Kinesiology, 7(4), pp. 241-250.
[16] T. Moritani, M. Muro and A. Nagata, 1986. "Intramuscular and surface electromyogram changes during muscle fatigue". Journal of Applied Physiology, 60(4), pp. 1179-1185.
[17] J. Bruce Moseley, Frank W. Jobe, Marilyn Pink, Jacquelin Perry, and James Tibone, 1992. "EMG analysis of the scapular muscles during a shoulder rehabilitation program". The American Journal of Sports Medicine, 20(2), pp. 128-134.
[18] D. David Ebaugh, Philip W. McClure, and Andrew R. Karduna, 2006. "Effects of shoulder muscle fatigue caused by repetitive overhead activities on scapulothoracic and glenohumeral kinematics". Journal of Electromyography and Kinesiology, 16, pp. 224-235.
[19] McQuade KJ, Dawson J, and Smidt GL, 1998. "Scapulothoracic muscle fatigue associated with alterations in scapulohumeral rhythm kinematics during maximum resistive shoulder elevation". The Journal of Orthopedic and Sports Physical Therapy, 28(2), pp. 74-80.
[20] L. Lindstrom, R. Kadefors and I. Petersen, 1977. "An electromyographic index for localized muscle fatigue". Journal of Applied Physiology, American Physiological Society, 43(4), pp. 750-754.
[21] Weytjens JLF, and van Steenberghe D, 1984. "The effects of motor unit synchronization on the power spectrum of the electromyogram". Biol Cybern, 51, pp. 71-77.
[22] Finsterer J., 2001. "EMG-interference pattern analysis". J Electromyogr Kinesiol, 11, pp. 231-246.
[23] C.J. De Luca, 1984. "Myoelectrical manifestations of localized muscular fatigue in humans". Crit. Rev. Biomed. Eng., 11 (4), pp. 251-279.
[24] B. Maton, and D. Gamet, 1989. "The fatigability of two agonistic muscles in human isometric voluntary sub maximal contraction: an EMG study. II Motor unit firing rate and recruitment". Eur. J. Appl. Physiol., 58, pp. 369-374.
[25] A. Luttmann, M. Ja¨ger, J. So¨keland, and W. Laurig, 1996. "Electromyographical study on surgeons in urology, Part II: Determination of muscular fatigue". Ergonomics, 39, pp. 298-313.
[26] K. J. Bennie, V.M. Ciriello, P.W. Johnson, and J.T. Dennerlein, 2002. "Electromyographic activity of the human extensor carpi ulnaris muscle changes with exposure to repetitive ulnar deviation". Eur. J. Appl. Physiol., 88, pp. 5-12.
[27] J. S. Petrofsky, 1979. "Frequency and amplitude analysis of the EMG during exercise on the bicycle ergometer". Eur. J. Appl. Physiol., 41, pp. 1-15.
[28] Basmajian JV, and DeLuca CJ., 1985. Muscle alive: their functions reviewed by electromyography. Williams & Wilkins, Baltimore.
[29] H. Westerblad, J. A. Lee, J. Lannergren and D. G. Allen, 1991. "Cellular mechanisms of fatigue in skeletal muscle". AJP - Cell Physiology, American Physiological Society, 261(2), pp. C195-C209.
[30] D. G. Allen and H. Westerblad, 2001. "Role of phosphate and calcium stores in muscle fatigue". Journal of Physiology, 536.3, pp. 657–665.
[31] Haken Westerblad, David G. Allen, and Jan Lannergren, 2002. "Muscle Fatigue: Lactic Acid or Inorganic Phosphate the Major Cause?". News in Physiological Sciences, The American Physiological Society 17(1), February, pp. 17-21.
[32] P. Zhou, N. L. Suresh, M. M. Lowery, and W. Z. Rymer, "Nonlinear Spatial Filtering of Multichannel Surface Electromyogram Signals During Low Force Contractions," IEEE Transactions on Biomedical Engineering, Vol. 56, No. 7, pp. 1871-1879, July 2009.
[33] Standards for Reporting EMG data. Journal of Electromyography and Kinesiology, February 1999; 9(1): III-IV.
[34] J. H. Semmlow, "Biosignal and Biomedical Image Processing: MATLAB-Based Applications," Marcel Dekker, Inc., New York, 2004, Ch. 3., pp. 79-162.
[35] Hubbard B. B., "The World According to Wavelets," 2nd ed., A.K. Peters, Ltd., Natick, MA, 1998.
[36] "Signal Processing Toolbox™ User's Guide," The MathWorks, Inc., 2010.
[37] Marple, S.L. Digital Spectral Analysis, Englewood Cliffs, NJ, Prentice-Hall, 1987, pp. 373-378.
[38] Schmidt, R.O, "Multiple Emitter Location and Signal Parameter Estimation," IEEE® Trans. Antennas Propagation, Vol. AP-34 (March 1986), pp.276-280.
[39] Johnson, D. H. and Dudgeon, D. E., "Array Signal Processing: Concepts and Techniques," Prentice-Hall, Englewood Cliffs, NJ, 1993.
[40] P. Kumar, A. Sebastian, C. Potluri, A. Urfer, D. S. Naidu, and M. P. Schoen, "Towards Smart Prosthetic Hand: Adaptive Probability Based Skeletal Muscle Fatigue Model," 32nd Annual International Conference of the IEEE Engineering in Medicine and Biology Society, Buenos Aires, Argentina, Aug. 31 – Sept. 4, 2010.